Development of a corrosivity classification for cement grouted cable strand in underground hard-rock mining excavations

by E. Villaescusa*, R. Hassell*, and A.G. Thompson*

Synopsis

A systematic study of groundwater conditions at eight underground mine sites exhibiting a wide range of groundwater qualities throughout Australia has been completed at the WA School of Mines. This has resulted in a new corrosivity classification for groundwater driven corrosion processes for cement grouted cable strand used in the Australian underground mining industry. The new corrosivity classification is simple to use and corrosion rates may be predicted from readily obtained *in situ* measurements of groundwater dissolved oxygen.

Introduction

The corrosion of rock reinforcement and support systems and the effect on their load bearing capacities has not been widely researched and is generally not well understood. While there is much literature relating to the phenomenon of corrosion, it is not always applicable to the hard-rock underground mining environment. Corrosion reduces the capacity and life expectancy of ground support, creating a number of safety concerns and operational difficulties in underground mining (see Figure 1).

Environmental conditions in Australian underground mines

A comprehensive data collection survey of environmental variables within eight Australian underground mines was undertaken within this project (Hassell *et al.*, 2004). The locations of the mines are shown in Figure 2.

A Corrosion Assessment System (Hassell, 2007) was used to collect a wide variety of information at numerous locations within each underground mine. While only specific locations were examined, they were selected to ensure an accurate representation of the different environments within a mine.

As part of the data collection, the key atmospheric variables were collected at every site. These included the quality of the ventilation, whether it was fresh air or part of the mine exhaust, its flow rate, and if there was an observable level of particulates. The wet and dry bulb temperatures were measured using a hygrometer from which the relative humidity was calculated.

If groundwater was present in sufficient quantities to be collected, it was analysed *in situ* using a portable TPS 90-FLMV field device (www.enviroequip.com.au). This analysis provides measurements of groundwater temperature, pH, dissolved oxygen levels and TDS concentrations. The source of the water, whether a fault, joint, borehole or a combination is noted, along with the rate of flow. The flow rate was described qualitatively using nomenclature from the rock mass rating classification (Bieniawski 1989). Samples of groundwater were also collected and assayed in a laboratory to determine the concentration of dissolved ions. Often the groundwater flow was not sufficient to collect an adequate sample. These regions were classified as wet if some water flow was occurring or damp if water is present but there are no signs of dripping or actual flow.

The underground mines studied displayed a large range in the values of groundwater variables such as TDS, pH, dissolved oxygen, temperature and the dissolved ionic species. Table I displays the average of the variables that were measured *in situ* at all mine sites. Variability with groundwater quality on a local mine scale is seen and also regional trends could be observed.

The rate of groundwater flow varied from site to site within a mine with the majority classified as either damp or wet with the only flowing water occurring in few large scale faults. Some areas showed evidence through

* *CRC Mining, WA School of Mines, Kalgoorlie, Western Australia.*

Journal Paper

Figure 1—Severely corroded cement grouted cablebolt

Figure 2—Location of assessed underground mines

Table I

Average *in situ* groundwater measurements at Australian underground mines

Mine site	TDS mg/ℓ	pH pH units	Dissolved oxygen mg/ℓ	Temperature °C
A	203 416	6.20	1.89	19.2
B	2 610	7.8	4.02	30.0
C Aquifer 1	4 540	7.39	5.55	19.7
C Aquifer 2	66 500	6.99	3.22	20.6
D	7 860	7.5	4.13	33.0
E Aquifer 1	47 250	7.3	4.35	26.5
E Aquifer 2	97 933	7.35	2.93	26.5
F	99 936	7.06	3.23	23.0
G Aquifer 1	12 260	8.30	3.53	28.6
G Aquifer 2	49 750	7.23	2.48	29.2
H Aquifer 1	44 000	7.40	3.13	24.0
H Aquifer 2	97 800	7.03	3.09	20.5
I	185 197	7.38	2.98	20.5
J	4 140	7.28	4.42	27.3

salt deposition of previous groundwater flow. Using the borehole camera it was observed that some of these areas still contain some groundwater away from the excavation boundary and were classed as damp.

The pH of the natural mine groundwaters sampled had a pH range of 6.20 to 8.30, which varies only slightly from neutral, at pH 7. The temperature of the groundwaters in the sampled Australian mines ranged from 14.6°C to 33.0°C. Higher temperatures were seen in mines in eastern Australia, due to the higher ambient rock temperatures, a product of the younger geological age of the region.

The dissolved oxygen concentration ranged in values from a low of 1.89 mg/ℓ at Mine A to a high of 5.55 mg/ℓ within Mine C Aquifer 1. The solubility of oxygen in water is a function of temperature and salinity. A comparison of the measured dissolved oxygen at the mine sites and the calculated dissolved oxygen from the temperature and salinity (Kester, 1975) is shown in Figure 3. The experimental results show that both higher temperatures and salinity will reduce the dissolved oxygen content.

Simulated underground environment

Six corrosion chambers (Figure 4) were designed and constructed to simulate the corrosive environments of the underground mines under consideration. This allowed long-term studies of corrosion rates for different reinforcement materials under controlled experimental conditions (Hassell *et al.*, 2006).

The testing to be carried out required a large volume of space that could not be provided by commercially available corrosion chambers. Therefore, it was decided to construct a set of purpose built units (2 m wide, 2.5 m long and 2 m high).

Each chamber had its own independent instrumentation unit, located on the outside of the chambers and connected directly to a humidifier and a heat lamp. Variations in the

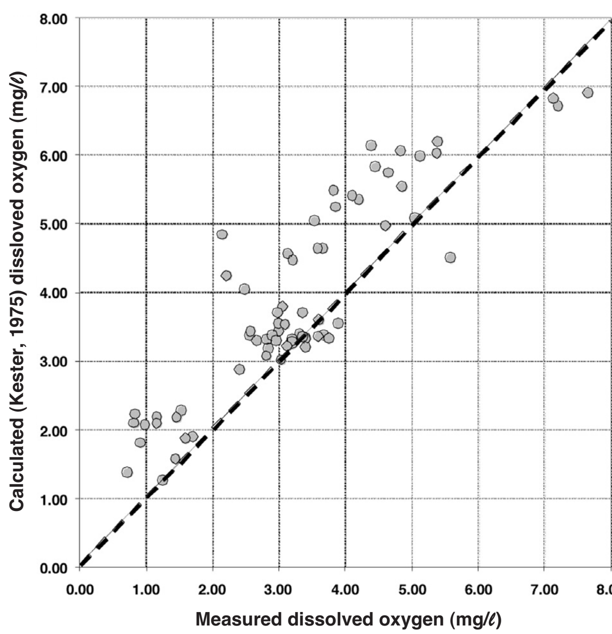

Figure 3—Calculated dissolved oxygen (Kester, 1975) compared to actual measured concentrations

Figure 4—A typical WASM corrosion chamber experiment

temperature of ±2°C and humidity ±5% from the set average caused the processing unit to either turn on or off the heat lamps and humidifier, keeping the atmospheric conditions within a set range.

Groundwater was collected directly from the rock masses of underground mines and transported to the corrosion chambers. An electric pump was used to propel the water through purpose built reticulation. This produced a constant supply of dripping or flowing groundwater being applied to the reinforcement and support being tested. The water flowed back into the rubber lined sump and was recirculated.

The groundwater was periodically analysed using a portable water analyser that gave immediate readings of the temperature, pH and dissolved oxygen. When the conditions departed from the underground situation the water was changed. The mean values and standard deviations for each constituent over the length of the experiments are shown in Table II. The variations in water properties occur for a number of reasons. The temperature of the water is controlled by the atmospheric temperatures; any change in it will affect the groundwater, which has a flow on effect to the dissolved oxygen. Rises in salinity were observed over time due to evaporation of the water and concentration of the dissolved ions. This again subsequently affected the dissolved oxygen. Of the measured parameters only the pH had little variation.

The groundwater collected from the participating mine sites had to be replenished as water was being lost from the corrosion chamber systems. As groundwater from the same aquifer displays variations in constituents, each batch of supplied groundwater was found to be slightly different.

Before any new groundwater was added to the chambers it was first analysed to make sure it was comparable. At two mines it was not possible to collect groundwater from the same location. At Mine D a rock fall prevented re-entry and at Mine H the area had been mined out and ventilation was not adequate for entry. At Mine C it was decided to change the groundwater as it had recently been intersected in deeper development excavations and was of greater interest to the mine.

Results for cement grouted cable strand

Cement grouted reinforcement is commonly used in Australian underground mines for its high load transfer capacity and resistance to corrosion damage. This resistance is provided by the protective alkaline environment of the cement grout and the physical barrier it provides from the surrounding environment. Experience, however, has shown that corrosion begins once the cement grout barrier is removed. This occurs by cracking of the grout column due to ground movement, blast damage, or in sections where the element is exposed from inadequate installation.

In an effort to better understand the response of cement grouted strand to corrosion attack following cracking of the grout column and infiltration of groundwater, a variety of strand combinations were placed within the six corrosion chambers.

Cable bolts utilized within the Australian mining industry commonly use a seven-wire, stress relieved, high tensile steel strand with plain (round) wires. Six wires are laid helically around a slightly larger diameter central (king) wire. The regular 15.2 mm diameter strand can be produced to provide a number of grades that provide differing yield and ultimate load capacities. Standard strand has a minimum yield force capacity of 213 kN and a minimum breaking force of 250 kN. Plain and bulbed strand cablebolts were tested.

The methodology used to investigate the load capacity of the cablebolt elements under corrosive conditions is the split pipe testing system (Villaescusa *et al.*, 1992). The elements were pull tested at periodic intervals to determine how corrosion affects the reinforcement effectiveness with time for different environments. The system is shown in Figure 5 and consists of two 500 mm long, galvanized, 68 mm diameter pipes that have been temporarily welded together at the split, which simulates a geological discontinuity. Cement grout mixes made from Portland cement (included the Methocel additive—2g per kg of cement) and having a water cement ratio of 0.35 were mixed and pumped into the split-pipes using an MBT GP2000A grout pump.

Table II

Average groundwater quality for each corrosion chamber

Chamber	Temp (°C)		Dissolved oxygen mg/ℓ		pH pH units		TDS mg/ℓ	
	Ave	St dev	Ave	St dev	Ave	St dev	Ave	St dev
Mine A	26.42	3.19	1.72	0.39	7.32	0.22	172 000	8 474
Mine C	26.28	2.01	3.17	0.50	7.69	0.46	37 644	17 046
Mine D	32.68	4.42	3.44	0.67	7.36	0.78	18 630	9 591
Mine F	26.24	1.92	2.48	0.39	7.27	0.78	79 200	15 651
Mine G	26.29	2.24	3.76	0.40	7.48	0.49	14 782	2 899
Mine H	27.10	4.27	2.78	0.54	7.82	0.26	38 005	7 862

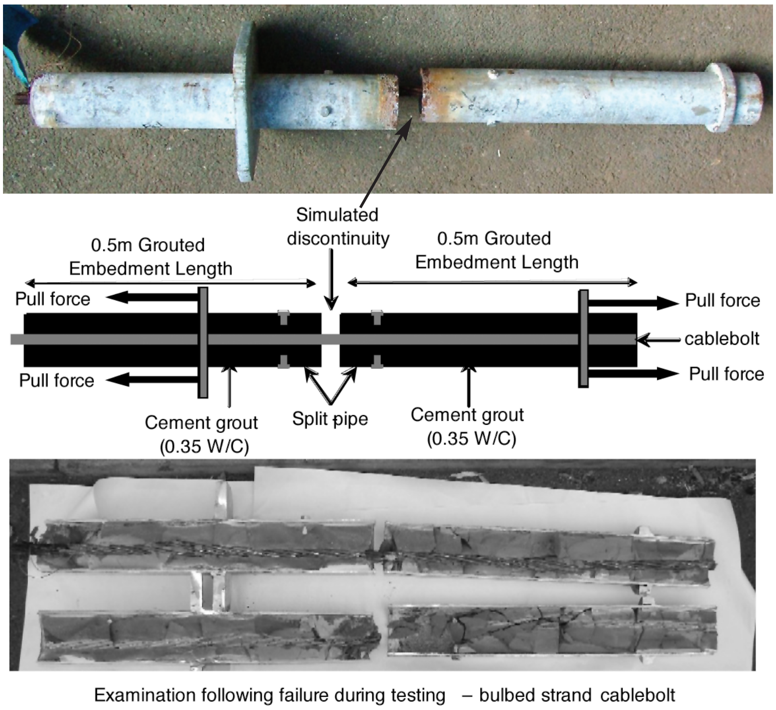

Figure 5—Schematic of the split-pipe testing system

To examine the effect of corrosion over time, each specimen was routinely tested using a 50 ton hydraulic Avery machine type 7110 DCJ. A maximum load of 170–175 kN for the cablebolt strand elements or a maximum displacement of 10 mm, whichever came first, was applied in all tests. These loads are well below the tensile strength of the elements, thus any failure could be attributed to the corrosion damage. Also, load transfer over an embedment length of 0.5 m means that the plain strand elements would not be able to utilize its full capacity, therefore for each test a 10mm limit was placed on the maximum displacement. This was to ensure that the specimens could be retested following more time under corrosive conditions in the chambers.

Pull testing of the split pipes was undertaken initially after intervals of 6 months in the corrosion chambers. Following the 733 day test due to failure of some elements the interval was reduced to 3 months. Pull testing was therefore conducted at 181 days, 361 days, 546 days, 733 days, 837 days, 922 days, 1 034 days and 1 132 days. Failure of the strand was characterised by breaking of one to six of the outside wires.

The evolution of corrosion damage from non-corroded to severe corrosion is shown in Figure 6. The non-corroded state occurs when the crack is initially opened and the grout cover is removed. The application of groundwater to the exposed strand creates increasing levels of corrosion damage culminating in failure, generally when severe corrosion damage has occurred. Severe corrosion damage is characterized by strong pitting corrosion around the circumference of the exposed strand reducing the cross-sectional area of steel and thus the tensile strength of the element.

It was noted that prior to the 181 day test no significant corrosion had occurred on the cable strands. This was a product of insufficient opening of the crack combined with

Figure 6—Stages of corrosion damage of cablebolt strand elements

self-healing of the grout preventing water ingress. The research concluded that at least 2 mm crack width is needed for before significant corrosion occurs. No statistical variation between the plain and bulbed strand information could be determined, hence the data was grouped by corrosion chambers. The data illustrate the tendency for failures to occur during similar time periods for specimens from the same corrosion chamber. This implies that the different environmental conditions in each chamber affect the rate of corrosion differently and therefore failure times.

Calculation of corrosion rates

The most widely used and simplest method of corrosion monitoring involves the exposure and evaluation of corrosion rates in actual test coupons (Dean and Sprowls 1987). Hence, on this study test coupons were placed in each corrosion chamber in order to compare the corrosivity of each simulated environment.

The preparation, placement, cleaning and evaluation of the corrosion coupon specimens was conducted to ASTM standard G4 that was designed to provide guidance for this type of testing (ASTM G1-90 1999). The coupons were obtained from a hot-rolled sheet of carbon steel grade HA300. The 1000 x 2000 x 0.6 mm sheet was guillotined into rectangular test specimens of 120 x 30 x 0.6 mm dimensions. Two 2 mm diameter holes were drilled in the upper left and right corners for the identification tags to be attached following measuring and weighing. To ensure an exact and reproducible finish, each coupon was sandblasted using silica grit. The coupons were then rinsed with distilled water, followed by acetate, which was cleaned with tissue paper; the coupons were allowed to dry on paper towels.

Following the drying process each coupon was measured to the third significant figure and weighed to the fifth significant figure. The identification tags, which were uniquely designed to survive the corrosive conditions, were attached to the coupon with cable ties (See Figure 7). The coupons were attached to the dripping reticulation (under strong water flow) within each corrosion chamber.

The coupons were tested for mass loss at 94 days, 180 days and 282 days. The corresponding rates of corrosion are shown in Table III. The reduction in the rate of corrosion over time for each chamber was reasonably constant. On average, reductions in the corrosion rate from the 94 day to the 180 day test by a factor of 1.34 and from the 94 day to the 282 day test, a reduction factor of 2.26 was calculated. These reduction factors were used to extrapolate data for some of the chambers where the coupons were completely oxidized by the 180 day test. These estimated results are shown (in italics) in Table III and denoted by dashed lines in Figure 8.

In general there is a reduction in the rates over time as the products of corrosion, the iron oxides, protect to some extent the underlying steel from further corrosion. This reduction becomes less pronounced with increasing exposure times and long-term corrosion rates can be established. The length of time needed to establish the long-term rate is dependent on the environment, but approximately 200–300 days are required.

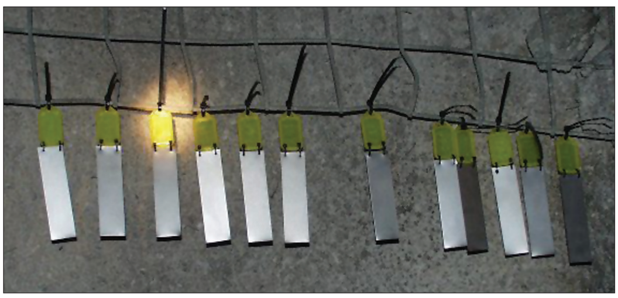

Figure 7—Typical test coupon geometry and placement

WASM groundwater corrosivity classification

A review of the existing corrosion classifications revealed that none adequately fits the experimental data and could not be readily used to predict the corrosivity of groundwater-affected environments examined in this study (Hassell, 2007). It was therefore necessary to examine each of the main groundwater properties individually to ascertain their influence. Given that the corrosion of steel is largely independent of pH values ranging between 4 and 10 and that

Table III

Corrosion rate from coupons in the corrosion chambers

Chamber	Corrosion rate (mm/y)			Groundwater
	94 days	180 days	282 days	flow
Mine D	1.32	*0.99*	0.58	Strong flow
Mine G	1.19	*0.90*	0.53	Strong flow
Mine C	0.85	0.67	0.38	Strong flow
Mine F	0.41	0.31	0.20	Strong flow
Mine H	0.33	0.24	0.12	Strong flow
Mine A	0.08	0.05	0.04	Strong flow

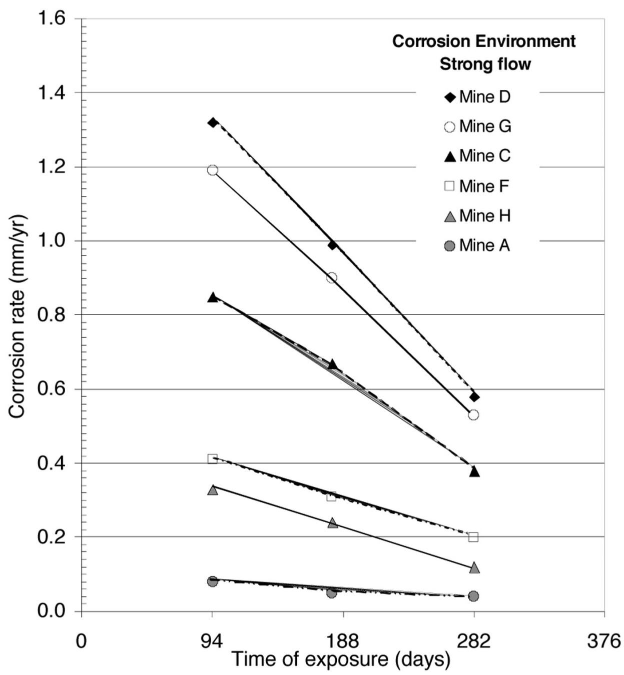

Figure 8—Measured and extrapolated corrosion rates for each corrosion chamber

all the natural groundwaters sampled had a pH in the range of 6.2 to 8.3. Therefore, it was assumed that pH has limited effect within this study. The remaining properties, temperature, TDS and dissolved oxygen, were examined to assess the data collected by the coupons placed within the corrosion chambers.

Temperature

A narrow range of temperatures was measured during the study and the corrosion chambers were set accordingly. The data show that no relationship between the corrosion rate and the average temperature (Figure 9).

Total dissolved solids

A good exponential relationship exists between the TDS of the water and the corrosion rate (Figure 10). The higher TDS waters result in a lower corrosion rate, presumably as the higher TDS waters reflect a lowering dissolved oxygen concentration.

Dissolved oxygen

A very good direct linear relationship that exists between the dissolved oxygen and the measured corrosion rates is displayed in Figure 11. Dissolved oxygen content has already been shown in Figure 3 to be directly related to the temperature and salinity of the water. Thus with one parameter all three controlling variables are taken into account. The good correlation with the TDS and the corrosion rates is partly due to the temperature values being similar and having a comparable effect on the corrosion rate.

Time

In general, a reduction in the rate of corrosion over time was observed. This is due to the corrosion products partly inhibiting further corrosion. This rate becomes constant after a certain period of time, dependent upon the environmental conditions. The information presented in Figure 12 is of the coupon test data from the corrosion chambers against the dissolved oxygen content, which remained more or less constant for the duration of the test.

The Mine A chamber had a decrease of 50% in the rate of corrosion from the 94 day test to the 282 day test with the Mine F chamber showing a 51% decrease and Mine H chamber a 64% decrease over the same time period. This

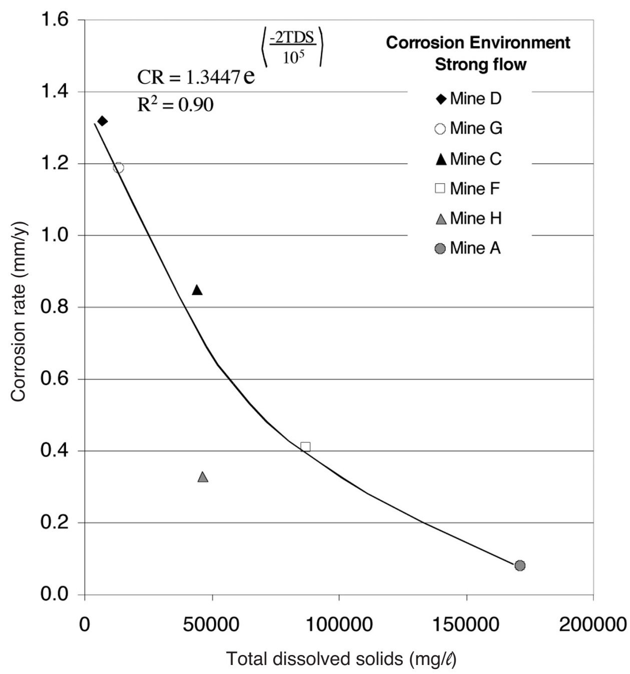

Figure 10—Total dissolved solids vs. corrosion chamber corrosion rates

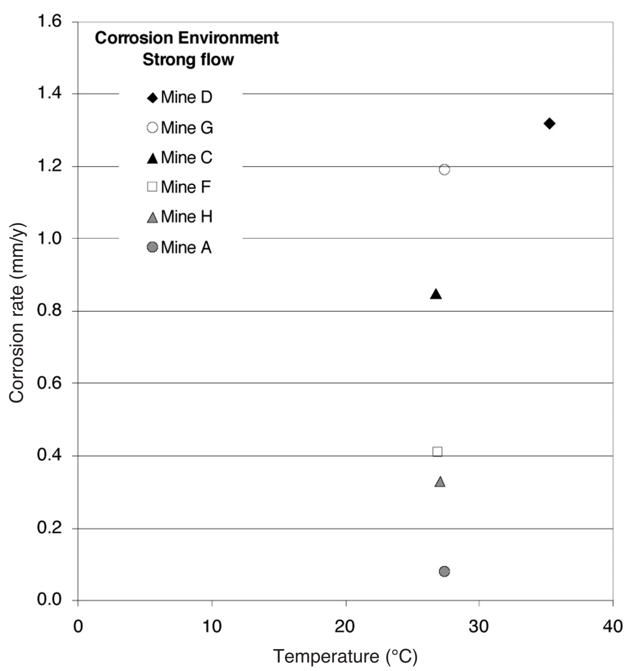

Figure 9—Groundwater temperature vs. corrosion chamber corrosion rates

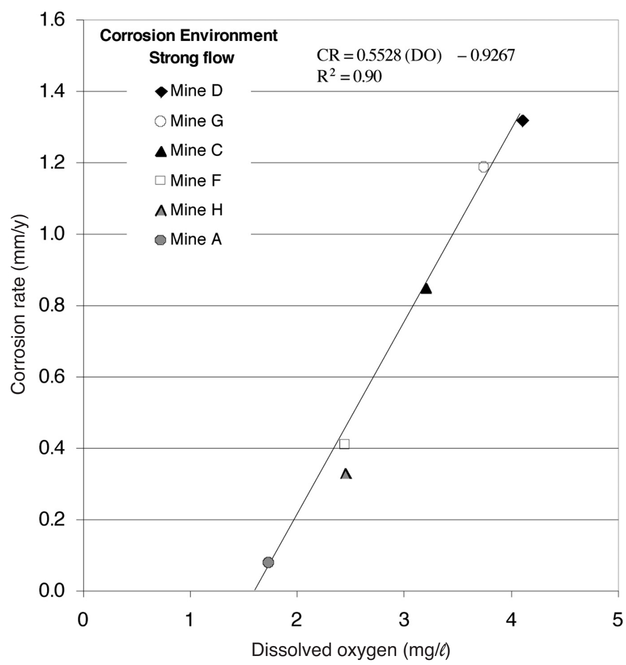

Figure 11—Dissolved oxygen vs. corrosion chamber corrosion rates

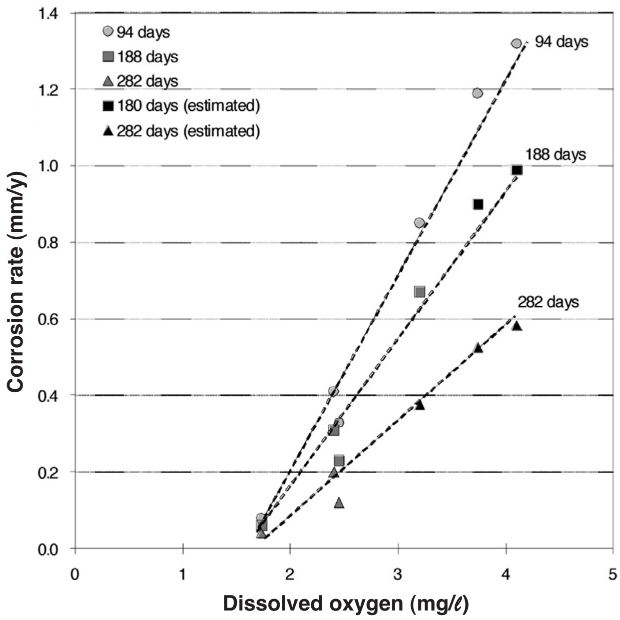

Figure 12—Measured and extrapolated corrosion rates over time

represents a relatively constant reduction for the different groundwater types. Coupon results that were not obtainable from these test periods due to high corrosion rates fully consuming the steel have been estimated (Table III). The calculated 282 day rate is representative of the long-term corrosion rate.

Flow rate

The rate of groundwater flow affects the corrosion rate by two processes. Increases in the flow rate simultaneously increase the rate at which dissolved oxygen is brought in contact with the steel surface. This provides more available oxygen for the electrochemical process and thus higher rates of corrosion occur. Higher flow rates also increase the level of physical erosion of the corrosion products and reduce the thickness of the partially protective cover increasing the corrosion rate.

To investigate the effect of flow rate, the coupon test results conducted at the mine sites, which had various rates of flow, are compared with those of the corrosion chambers. The water properties are comparable and a similar time of exposure periods is examined. Coupons from the Mine A chamber (flowing) had a higher corrosion rate by a factor of 3.5–4 times that of the mine site results (wet). Similarly, the Mine H chamber results (flowing) had a higher corrosion rate by a factor of 2.5–3 compared with the field results for a wet rock mass and 4.5 time increase compared to a damp rock mass.

If all the long-term corrosion rates, for both the corrosion chambers and field tests are plotted against dissolved oxygen, they can be grouped based on their respective groundwater conditions, as shown in Figure 13.

Corrosivity for groundwater affected hard rock environments

Table IV shows a newly proposed classification for groundwater affected, hardrock conditions found in Australian underground mines. The new proposed classification is based on the comprehensive data collection survey and the calculation of corrosion rates by coupon testing undertaken as part of this study. The classification considers two factors in determining the corrosivity of the groundwater: dissolved oxygen content as measured *in situ* from a dissolved oxygen probe and the groundwater flow conditions as described in Figure 13. Uniform corrosion rates for HA300 grade steel can then be estimated for different environments.

The classification provides a range of possible corrosion rates for a specific dissolved oxygen content and groundwater flow. As the groundwater condition is from qualitative observation rather than quantitative assessment, this variation in values is necessary. Projection of the corrosion rates for measurements of dissolved oxygen less

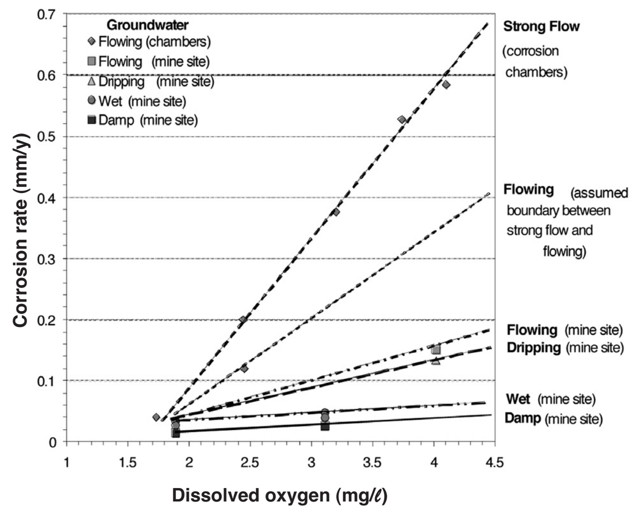

Figure 13—Rate of corrosion in coupons grouped by groundwater flow

Table IV

Maximum corrosion rates for HA300 steel in groundwater affected Australian hard rock mining environments

Strong flow—large continuous water flow from a large fault of many fractures				
Dissolved oxygen (mg/ℓ)	1–2	2–3	3–4	4–5
Corrosive rate (mm/y)	<0.12	0.12–0.36	0.36–0.58	0.58–0.8
Flow—water flows form fractures				
Dissolved oxygen (mg/ℓ)	1–2	2–3	3–4	4–5
Corrosive rate (mm/y)	<0.09	0.090–0.225	0.225–0.365	0.365–0.50
Dripping—numerous drips and trickling of water from fractures				
Dissolved oxygen (mg/ℓ)	1–2	2–3	3–4	4–5
Corrosive rate (mm/y)	<0.06	0.060–0.105	0.105–0.160	0.16–0.20
Wet—rock mass discoloured. Dripping from fractures moderately common				
Dissolved oxygen (mg/ℓ)	1–2	2–3	3–4	4–5
Corrosive rate (mm/y)	<0.04	0.040–0.075	0.075–0.100	0.10–0.12
Damp—rock mass is discoloured from dry rock mass. Very minor drips				
Dissolved oxygen (mg/ℓ)	1–2	2–3	3–4	4–5
Corrosive rate (mm/y)	<0.02	0.020–0.030	0.030–0.040	0.04–0.05

than 1.5 and greater than 4.5 is uncertain due to insufficient data. The given corrosion rates are for uniform corrosion only; it is, however, appropriate to assume that pitting corrosion will increase with higher rates of uniform corrosion. The classification does not take into account the rock mass quality. It is assumed that if the classification is to be applicable, the reinforcement will intersect water-bearing discontinuities. In addition, the rock mass damage from the stress redistribution is expected to increase the permeability within the zones where reinforcement is utilized.

Implications for cement grouted cable strand

In mass mining, cable bolt systems are used to reinforce large blocks or wedges often in long life excavations. Premature failure of these reinforcement systems due to corrosion can cause significant safety and operational issues. It is strongly recommended that best practice installation requirements such as those detailed by Windsor (2004) and Hassell *et al.*, (2006) are followed to minimize the potential for corrosion damage to occur.

Approximate minimum and maximum service lives have been measured from the corrosion chamber experiments. The service life is estimated as the material loss required to cause failure of the strand loaded to 175 kN or approximately 17.5 tons, a 30% decrease in the original capacity of 250 kN. Groundwater is assumed to be present and it is assumed that either cracking of the grout column has occurred or grout encapsulation is poor. Comparing the measured service lives to the corresponding corrosion rates of the simulated environment calculated using the corrosivity classification, estimates can be made to the expected minimum and maximum service lives (<17.5 kN) of 15.2 mm diameter black strand across a range of corrosion rates and are shown in Figure 14.

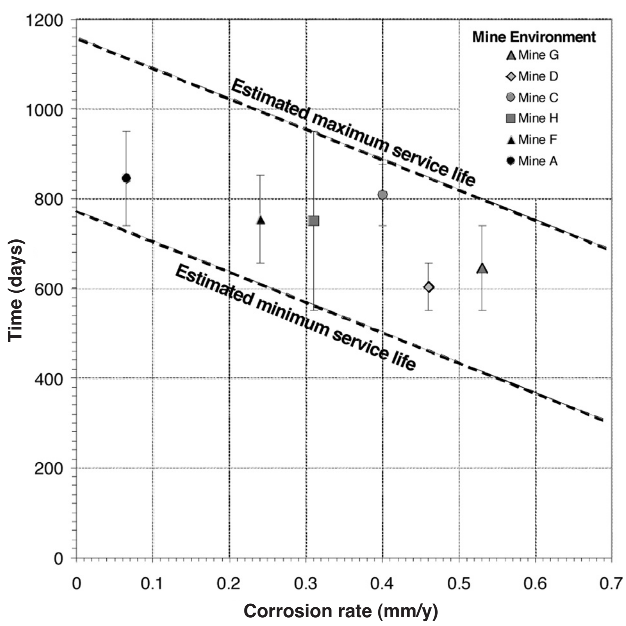

Figure 14—Service life estimates for cable strand in strong groundwater flow environments

It is estimated that even in the most corrosive conditions observed in underground mines cable strand will last at least one year once cracks along the element axis have formed. This figure is much higher than the expected life of uncoated barrel and wedge anchors, found to be approximately 7 months at comparatively corrosive conditions. It is recommended that barrel and wedge corrosion protection systems such as a long life lubricant at the barrel/wedge interface and barrier coatings are applied following installation (Hassell *et al.*, 2006).

Conclusion

The investigations presented here have resulted in the development of corrosion classifications for the Australian underground hard-rock mining environments and guidelines have been provided for the design of cement grouted cable bolt elements. This has been achieved through the completion of environmental characterization of a number of underground mines, laboratory testing using a simulated underground environment, examination of reinforcement elements *in situ* and the exposure and evaluation of test coupons to obtain corrosion rates for the underground mining environment

Acknowledgements

The authors wish to acknowledge the support of the Minerals and Energy Institute of WA (MERIWA), BHP Billiton, PlacerDome Asia Pacific, Xstrata Ltd, Barrick Gold Australia, GoldFields Australia, MBT (Australia) and Strata Control Systems.

The technical support of Mr. Brett Scott and Mr. Lance Fraser, WASM technicians is also gratefully acknowledged.

References

ASTM G1-90 (1999). Standard Practice for Preparing, Cleaning, and Evaluating Corrosion Tests Specimens. ASTM International.

Bieniawski, Z.T. *Engineering Rock Mass Classifications*, Wiley, New York. 1989.

Dean, S.W. and Sprowls, D.O. In-Service Monitoring, J.R. Davis (ed.), *Metals Handbook Ninth Edition: Corrosion*, vol. 13, ASM International, USA. 1987.

Hassell, R., Villaescusa, E., Thompson, A.G., and Kinsella, B. Corrosion assessment of ground support systems. *Procc. Ground Support in Mining and Underground Construction*, Villaescusa, E. and Potvin, Y. (eds.), Balkema, 2004. pp. 529–539.

Hassell, R. Corrosion of rock reinforcement in underground excavations, PhD Thesis, Curtin University of Technology, 2007. 274 pp.

Hassell, R., Villaescusa E., and Thompson, A.G. Testing and evaluation of corrosion on cablebolt anchors. *Procc. 41st US Rock Mechanics Symposium, 50 Years of Rock Mechanics—Landmarks and Future Challenges*, Golden Colorado. 2006.

Kester, D.R. Dissolved Gases Other Than CO_2, JP Riley & G Skirrow (eds.), *Chemical Oceanography*, 2nd edn, vol. 1, Academic Press. 1975.

Villaescusa, E., Sandy, M.P., and Bywater, S. Ground support investigations and practices at Mount Isa, *Procc. Rock Support in Mining and Underground Construction,* Kaiser and McCreath (eds), Balkema, 1992. pp. 185–193.

Windsor, C.R. A review of long, high capacity reinforcing systems used in rock engineering. *Procc. Int. 5th Ground Support in Mining & Underground Construction*, Villaescusa, E. and Potvin, Y. (eds.), Balkema, Perth, 2004. pp. 17–41. ◆